

# Chapter 4

## Advanced phase plane analysis

In this chapter, we build on our definition of the phase plane and the previous results and we introduce a finer description of all the phenomena that may happen for nonlinear systems. In particular, we now introduce a finer description of phenomena that may appear in nonlinear systems, such as limit cycles and separatrices. We also provide a more comprehensive study of equilibria, when the linearization procedure fails. Finally, we also talk about systems with discontinuous derivatives and/or hysteresis, as they are very common in aerospace applications.

### 4.1 Additional behaviors

#### 4.1.1 Limit cycles

##### Introduction

In the analysis of nonlinear systems, singular points are not the only interesting points that one may want to hunt for: many nonlinear systems, although unstable, exhibit *limit cycling*: although trajectories stay bounded, they experience sustained and repeated oscillations. A classical example of a system which exhibits limit cycling is the Van der Pol oscillator, which is an early electrical circuit obeying the dynamical

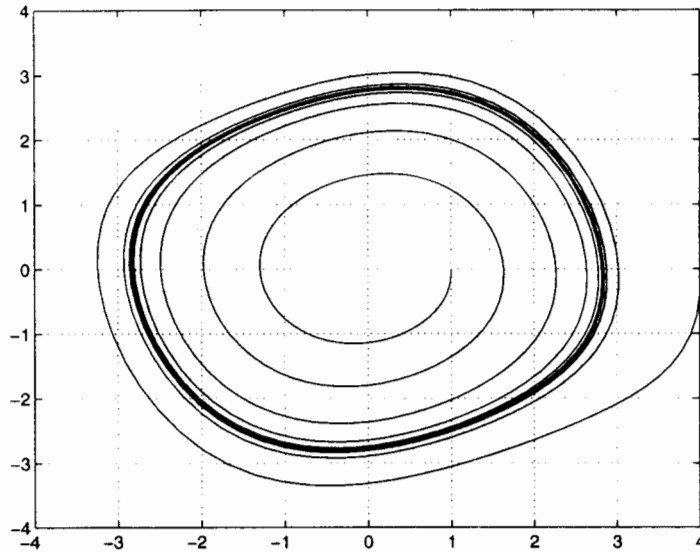


Figure 4.1: phase-plane trajectories for Van der Pol oscillator

equation

$$\ddot{y} - \epsilon(1 - y^2)\dot{y} + y = 0, \quad \epsilon > 0.$$

In Fig. 4.1, we have plotted (using canonical coordinates) the trajectories originating at the initial points  $(1, 0)$  and  $(4, 0)$ , respectively, with  $\epsilon = 0.1$ . As can be seen, after transients, both trajectories seem to converge to a closed curve, from inside and outside respectively. Such a closed curve is named *limit cycle*. Determining limit cycles is as important as finding singular points in the analysis of nonlinear systems.

Before proceeding further about performing this task, let us give (at least) one good reason why systems exhibiting limit cycles have significant engineering importance: in Fig. 4.2, we have plotted the value of  $x_1$  as a function of time for the vanderpol oscillator; as may be seen, eventhough it does not look *exactly* like a sinusoid, it looks very much like it. In fact, once passed through a low-pass filter, it *will be* a sinusoid. Thus, the Van der Pol oscillator may be viewed as a convenient *function generator*, that may be used, say, to get the transfer function of some linear system. This was actually used before the introduction of digital, highly flexible electronic components. Historical irony, where nonlinear systems contributed to make linear systems theory practical

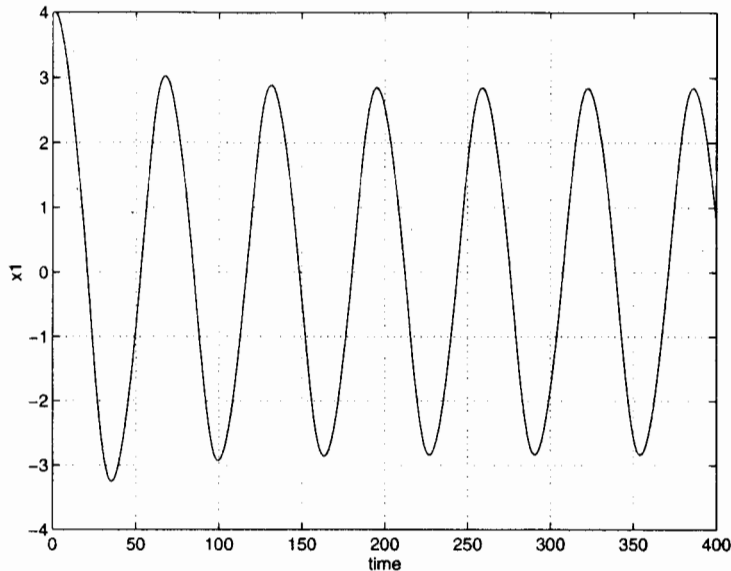


Figure 4.2: Output of Van der Pol oscillator

from an Engineering viewpoint! As for singular points, limit cycles may be stable, unstable, or both. For example, the limit cycle exhibited by the Van der Pol oscillator may easily be considered as stable, because the “distance” from the trajectories to the limit cycle tend to 0 as time tends to  $\infty$ . This limit cycle becomes unstable if one now plays the Van der Pol equation *backwards* in time. There also exist limit cycles which are stable *and* unstable. This is the case, for example, of the system given by the set of first-order differential equations

$$\begin{aligned}\frac{d}{dt}x_1 &= \left| \sqrt{x_1^2 + x_2^2} - 1 \right| \frac{x_1}{\sqrt{x_1^2 + x_2^2}} - x_2 \\ \frac{d}{dt}x_2 &= \left| \sqrt{x_1^2 + x_2^2} - 1 \right| \frac{x_2}{\sqrt{x_1^2 + x_2^2}} + x_1.\end{aligned}$$

whose limit cycle is the unit circle and whose outside trajectories tend to get away from this circle, whereas its inside trajectories get nearer this circle as time increases, as seen in Fig. 4.3. Some of the simplest limit cycles are neither stable nor unstable: trajectories of undamped mass-spring systems in the phase plane are ellipsoids parallel to each other, and each ellipsoid may be seen as a limit cycle (see Fig. 4.4). The limit

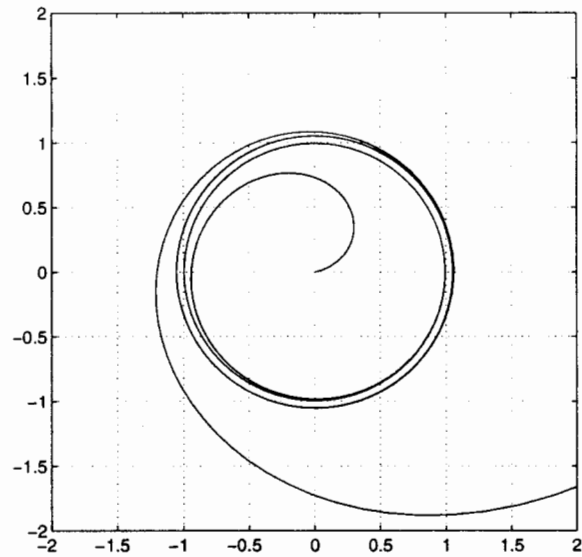


Figure 4.3: Stable-unstable limit cycle

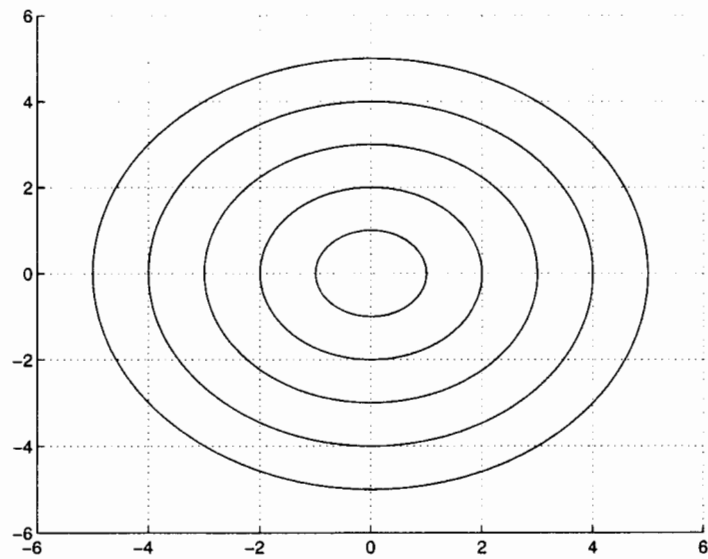


Figure 4.4: Undamped mass-spring system trajectories

cycle on which the system actually is only depends on its initial total energy (which stays constant). *Conservative systems* usually exhibit such behaviors, and they will be studied in more detail later on.

### Criteria for limit cycle determination

When analyzing limit cycles, there are two tasks to consider: first, we will discuss the question of *existence* of limit cycles in the phase plane. Second, we will also discuss the relation of limit cycles to singular points via *Poincaré's index theory*. We will also discuss clues that may lead to determining limit cycles.

The second task is then to determine *quantitatively* what the limit cycle looks like. The easy answer is to use computer simulation. The harder (and more general one) will be discussed later on.

- **Criterion for non-existence of limit cycles (Bendixson's first theorem)**

Consider the second-order system defined by

$$\begin{aligned}\frac{d}{dt}x_1 &= f_1(x_1, x_2) \\ \frac{d}{dt}x_2 &= f_2(x_1, x_2).\end{aligned}$$

Assume that in a subdomain  $\mathcal{D}$  of the phase plane, the quantity

$$\operatorname{div} f = \frac{\partial f_1}{\partial x_1} + \frac{\partial f_2}{\partial x_2}$$

has constant sign, then there can be no limit cycle, nor any closed trajectory in this domain. Indeed, let  $\Gamma$  be the boundary of  $\mathcal{D}$ . Then from Green's (or Gauss's) theorem, we have

$$\oint_{\Gamma} (f_1 dx_2 - f_2 dx_1) = \int \int_{\mathcal{D}} \operatorname{div} f dx_1 dx_2.$$

Thus, if  $\Gamma$  was a closed trajectory of the domain, then any point  $(x_1, x_2)$  of  $\Gamma$  would satisfy

$$\frac{dx_2}{dx_1} = \frac{f_2}{f_1} \text{ or } f_1 dx_2 - f_2 dx_1 = 0.$$

Thus a contradiction. Of course, a little more care has to be exercised during the (many) situations when  $f$  is nondifferentiable, or even discontinuous.

Note that we have mentioned the words “limit cycle”, as well as “closed trajectory”. This is to reflect that there exist trajectories in the phase-plane which are closed but are not limit cycles: consider for example the inverted pendulum satisfying the equation

$$\ddot{\theta} + \sin \theta = 0$$

Then, the two unstable equilibria  $(-\pi, 0)$ , and  $(\pi, 0)$  are connected by two trajectories, shown in Fig. 4.5. Such closed curves, although not limit cycles, are very important in the analysis of nonlinear systems, because they mark the *boundary* between two very different, qualitative behaviors of a dynamical system (complete the figure to illustrate this fact). Other names for such curves are *separatrices*. When encountering several equilibria (in particular stable and unstable ones), it is always a good idea to look for those specific trajectories that link unstable to stable equilibria.

#### • Poincaré indices

Consider the system

$$\begin{aligned} \frac{d}{dt}x_1 &= f_1(x_1, x_2) \\ \frac{d}{dt}x_2 &= f_2(x_1, x_2). \end{aligned}$$

Consider a closed curve  $\Gamma$  in the phase plane and a point  $M$  riding on  $\Gamma$  counterclockwise. Assume this curve goes through no singular point. Then, assuming  $f_1$  and  $f_2$  to be continuous, for all positions of  $M$ ,  $f_1$  and  $f_2$  are not simultaneously zero, such that it is legal to talk about the vector  $\tau$ , tangent to the trajectory passing through  $M$ . As  $M$  travels on  $\Gamma$ , the vector  $\tau$  rotates an integer number of times. This number is named *index of  $\Gamma$  with respect to the vector field*, and it is invariant under small variations of  $\Gamma$ . (Note the similarity between this index and what

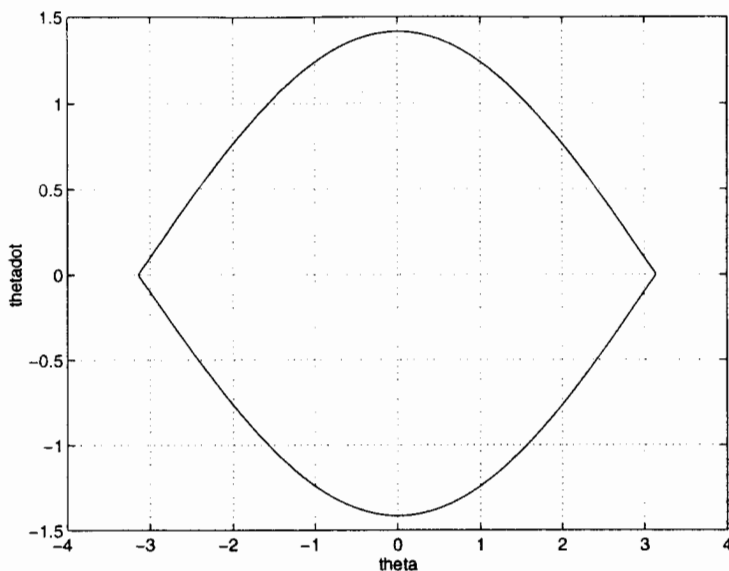


Figure 4.5: Closed trajectory for a pendulum

you learned regarding Nyquist stability criterion.) Depending on the type of singularities contained in  $\Gamma$ , the value of this index is going to vary. For example, the Poincaré index for any singular point which is either completely attractive, repulsive or neutral (pure imaginary eigenvalues) is equal to one, as illustrated in the first 3 pictures in Fig. 4.6. However, the reader may realize that the Poincaré index for a saddle point is equal to  $-1$  (see the last picture in 4.6). Thus, the Poincaré index is a characteristic number of a given singular point. When  $\Gamma$  contains many singular points, the index of  $\Gamma$  is the algebraic sum of all indices. Poincaré indices are very useful to get information about singular points and limit cycles. For example, if  $\Gamma$  turns out to be a limit cycle for the dynamical system, then its index is equal to 1. As a result, a limit cycle must always be around a singular point. If it contains only one singularity, it **MUST** be a node, or a focus, or a center. If it contains more than one, then the algebraic sum of indices has to be equal to 1; thus there must be an odd number of singular points, and if there are  $n$  saddle points, then there must be  $n + 1$  focuses and nodes.

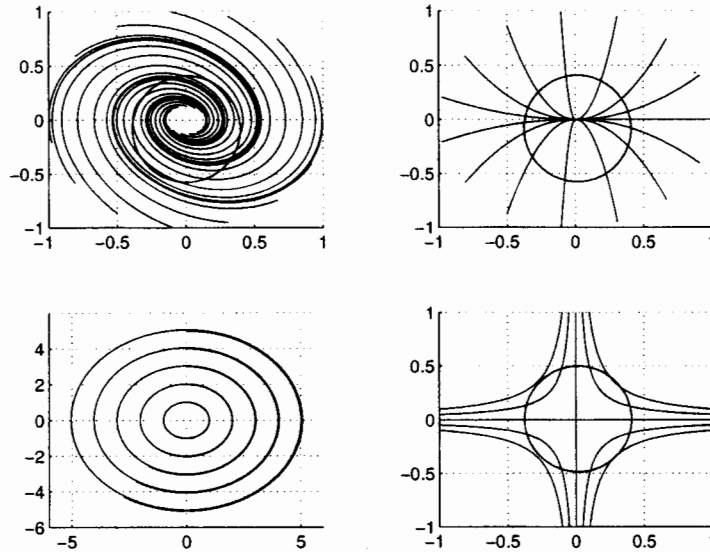


Figure 4.6: Poincaré indices for various singular points

Limit cycles are not necessary to determine existence of singular points: for example, assume there exists a closed curve  $\Gamma$  such that all trajectories cross it inwards (resp. outwards), as shown in Fig. 4.7. Then its index is equal to 1 and it must contain a singular point.

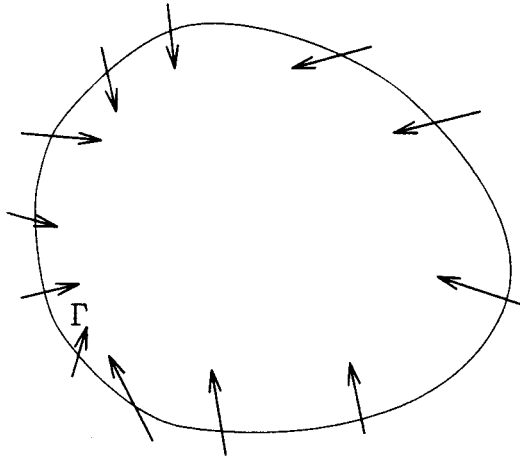
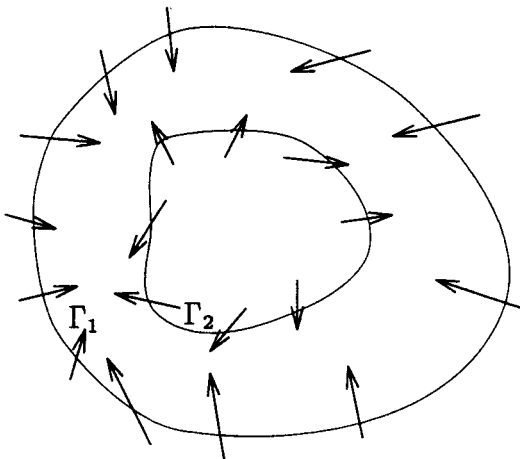
- **Clues for existence of limit cycles (Bendixson's 2nd theorem)**

Consider the dynamic system

$$\frac{d}{dt}x = F(x),$$

Assume it is possible to find two closed curves  $\Gamma_1$  and  $\Gamma_2$  such that (i)  $\Gamma_1$  contains  $\Gamma_2$ , and (ii) all trajectories crossing  $\Gamma_1$  cross it inwards and all trajectories crossing  $\Gamma_2$  cross it outwards as shown in Fig. 4.8. Then there exists at least one closed trajectory between  $\Gamma_1$  and  $\Gamma_2$ . Of course, this theorem does not tell us which type of closed trajectory we may actually encounter, but it definitely hints there may be a limit cycle there, which is likely to be stable, since all trajectories tend to enter the annulus



Figure 4.7: All trajectories cross  $\Gamma$  inwardsFigure 4.8: All trajectories cross  $\Gamma_1$  inwards,  $\Gamma_2$  outwards

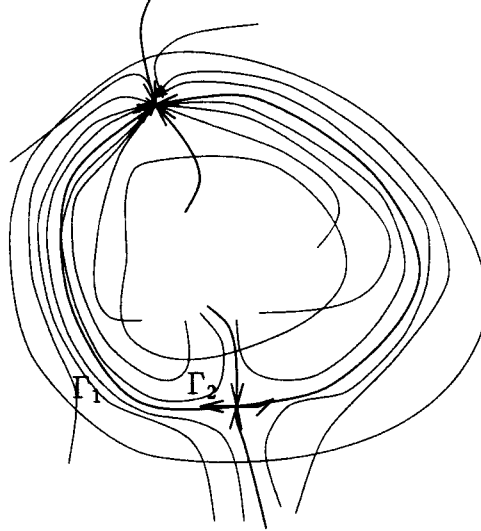


Figure 4.9: No limit cycle, yet a closed trajectory.

defined by  $\Gamma_1$  and  $\Gamma_2$ . However, this is not the only possibility, as shown in Fig. 4.9. We will find these concepts again later on, when studying stability of nonlinear systems in the sense of Lyapunov.

### 4.1.2 Singular points

In the previous chapter, we've seen that the study of many singular points may reduce to the study of the linearized system around this singular point. The limits of such an analysis are reached when one or two of the eigenvalues for the linearized system have zero real part, in which case many complicated behaviors may arise. The goal of this section is not to give a general theory to treat such cases, but rather to show you how messy things can be.

#### Examples

It is very easy to build a physical system that actually has a singular point and no linearization allows to conclude stability or instability. Consider for example the mass-spring system shown in Fig. 4.10. The mass is free to slide horizontally. When it is at 0, the springs are not

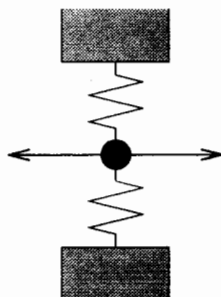


Figure 4.10: Nonlinear mass-spring system

extended. The mass may be subject to viscous friction, proportional to the square of the speed. Let the length of the springs at rest be equal to 1, the mass be also equal to 1. Assume finally that the spring stiffnesses are equal to  $1/2$ . Then the equations of motions for this system may be written as

$$\ddot{x} + \lambda \dot{x} + \frac{x^3}{(\sqrt{x^2 + 1} + 1)\sqrt{x^2 + 1}} = 0,$$

where  $\lambda$  is the friction coefficient. The linearized system around 0 is then

$$\ddot{x} + \lambda \dot{x} = 0,$$

which has either one or two poles at zero. This linearized model does not give us a single clue about the stability of the original system nor about the shape of the trajectories around 0. We actually need to rely on our physical knowledge of the system to tell that the system is stable. However, it is very hard to predict a “shape” for the trajectories around 0: while as seen from far away, the trajectories are such that 0 looks like a focus, a closer look suggests that 0 is actually a node, as seen on Fig. 4.11. Setting the drag coefficient  $\lambda$  to 0 also generates interesting behaviors, as can be seen in Fig. 4.12, where large amplitude limit cycles are almost ellipsoidal, whereas small amplitude limit cycles are oval shaped. Consider now the dynamical system given by the equation

$$\ddot{y} + y^2 = 0. \quad (4.1)$$

The corresponding phase portrait around 0 is shown in Fig. 4.13. In

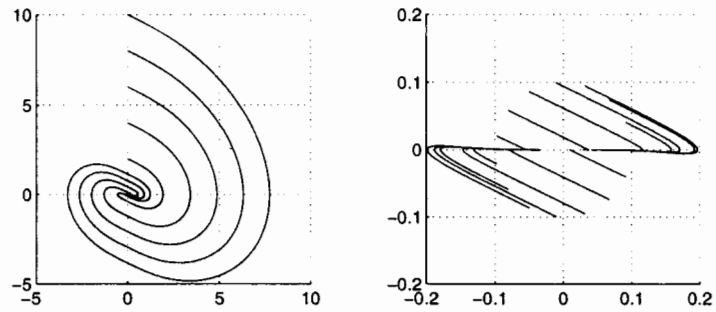


Figure 4.11: Nonlinear mass-spring system with drag

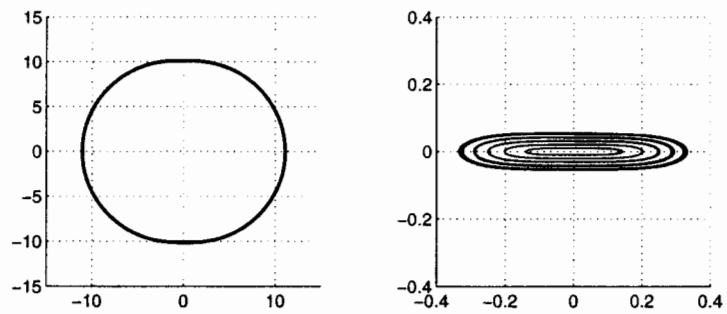
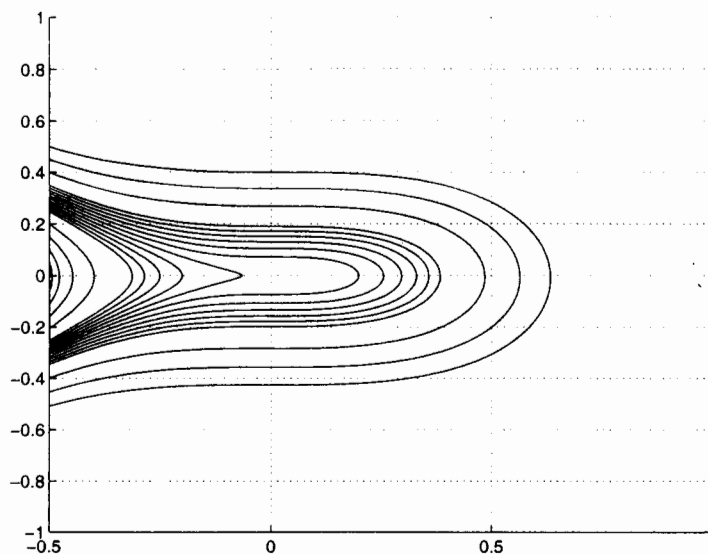


Figure 4.12: Nonlinear mass-spring system with no drag (Nota: trajectories should be closed, but aren't due to numerical errors)

Figure 4.13: Phase portrait for  $\ddot{y} + y^2 = 0$ .

particular, we see that the motion looks like a mix of a saddle point and a center (compute the index of this singular point?). Note that the trajectories of this system are easy to obtain (as for any conservative system, by the way). Indeed, it is possible to integrate (4.1) to obtain the equation

$$\dot{y}^2 + \frac{1}{3}y^3 = K.$$

Like saddle points, zero is simultaneously a stable and an unstable point. However, the trajectories going through 0 are now the two functions

$$\dot{y} = \pm \frac{1}{\sqrt{3}}y^{3/2}, \quad y \leq 0.$$

Once again, it helps understanding this system when remarking that it may represent the motion of a cart sliding on a curve shaped as shown in Fig. 4.14.

### General rules

The previous examples should convince you that there are few applicable rules as far as singular points corresponding to singular values

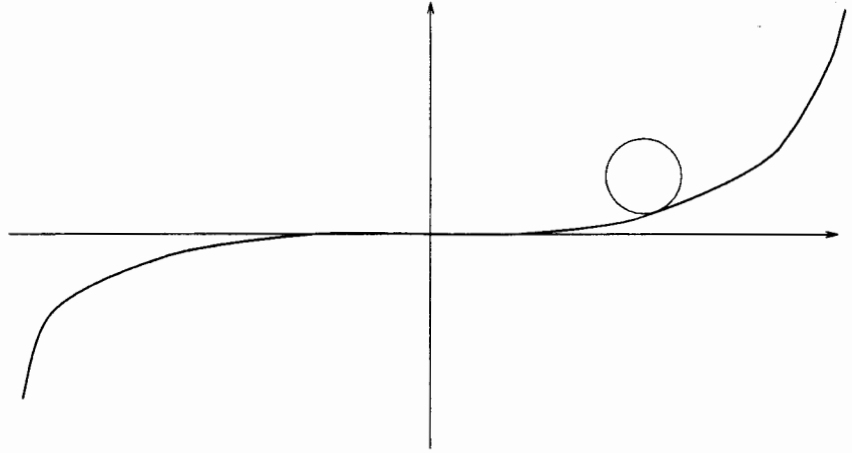


Figure 4.14: Cart on a slope.

with zero real part are concerned. The richness of possible behaviors is very large, and one needs to rely on intuition, simulation and physical insight to understand what happens.

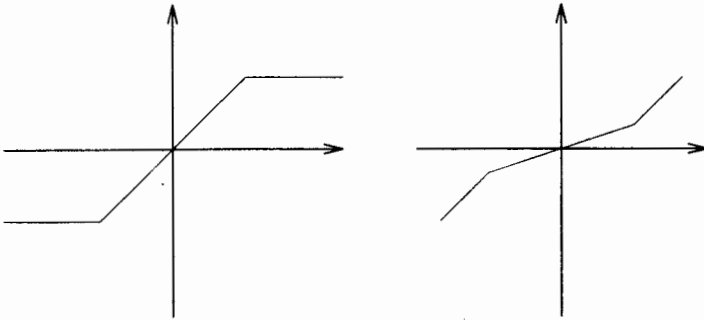


Figure 4.15: Left: saturation. Right: hardening gain

linear (they often are double integrators), but their actuation or sensory system is only piecewise linear. The singlemost encountered such nonlinearity is saturation, which is ubiquitous in airplanes (past 30 degrees, a control surface does not have much additional effect), and which is the cause for many troubles (PIOs in particular). A typical saturation characteristic is shown in the left of Fig. 4.15. In aircraft industry, the advent of digital electronics and Fly-By Wire control logic has contributed to the purposeful introduction of nonlinearities in the flight control systems, especially in the pilot loop. For example, nonlinearities such as hardening gains (as shown in the right of Fig. 4.15) have been under consideration for implementation in aircraft control loops. Once we know how to plot the phase portrait for *linear* systems, plotting the phase portrait for piecewise linear nonlinear systems is easy; consider for example the control of a double integrator via lead control and saturation (this is the case, say, for a satellite). The resulting equations of motion are

$$\ddot{\theta} + \text{SAT}(\theta + 0.2\dot{\theta}) = 0.$$

The corresponding phase plane is divided in three regions in which the system is fundamentally linear, and the dynamics for the system may be summarized as

$$\begin{cases} \ddot{\theta} - 1 = 0 & \text{whenever } \theta + 0.2\dot{\theta} \leq -1 \\ \ddot{\theta} + 0.2\dot{\theta} + \theta = 0 & \text{whenever } |\theta + 0.2\dot{\theta}| \leq 1 \\ \ddot{\theta} + 1 = 0 & \text{whenever } \theta + 0.2\dot{\theta} \geq 1. \end{cases}$$

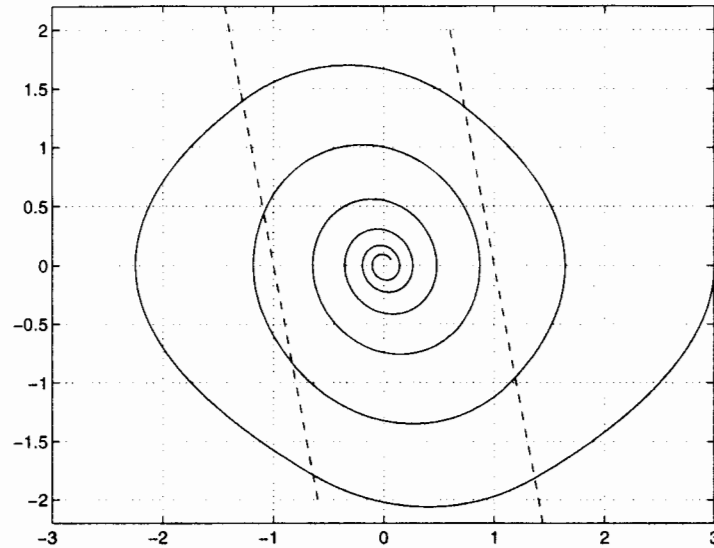


Figure 4.16: Phase portrait for saturating satellite control system.

Thus, the phase portrait for this system is made of a juxtaposition of parabolas and logarithmic spirals, separated by two lines, as shown in Fig. 4.16. Studying the stability properties of such systems is no more complicated than previously. Only care has to be exercised with isoclines across different regimes.

Another type of nonlinearity comes from systems where actuation is not symmetric: for example, some satellite systems are equipped with only one thruster (which therefore can push only in one direction) or two opposing thrusters with different characteristics. Using the same lead control law as earlier, the satellite dynamics are now going to be

$$\begin{cases} \ddot{\theta} + 0.5(0.2\dot{\theta} + \theta) = 0 & \text{whenever } \theta + 0.2\dot{\theta} \leq 0 \\ \ddot{\theta} + 0.2\dot{\theta} + \theta = 0 & \text{whenever } \theta + 0.2\dot{\theta} \geq 0, \end{cases}$$

if one thruster is assumed to work nominally and the other only produces half of what it is supposed to. In this case, there appears a piecewise linear discontinuity which stands right on top of the (presumed) equilibrium point 0, such as shown in Fig. pcwslinbis, and linearization techniques fail to characterize the stability properties of this equilibrium. We will see later on that general methods exist that *prove* stability of such systems, based on *Lyapunov stability theory*.



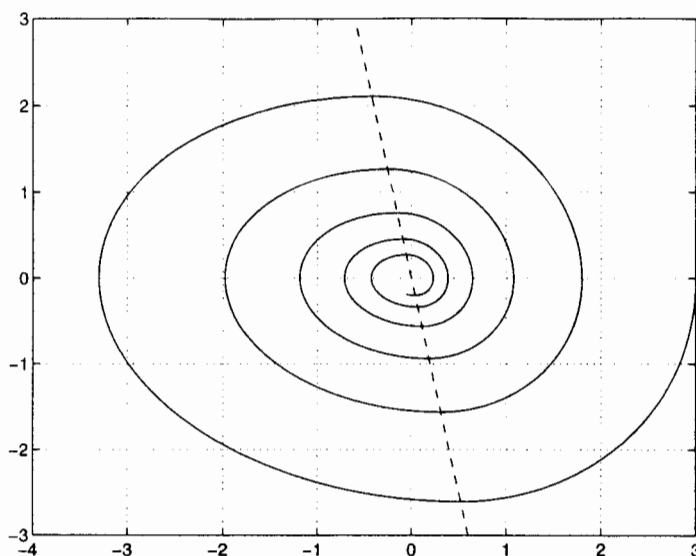


Figure 4.17: Phase portrait for asymmetric satellite control system.

### 4.2.2 Systems with piecewise linear, discontinuous nonlinearities

#### On-off control systems

This type of system turns out to be extremely common in aerospace applications, for reasons we will explain in the next chapter. In particular, the “switch” nonlinearity shown in Fig. 4.18 is a big favorite

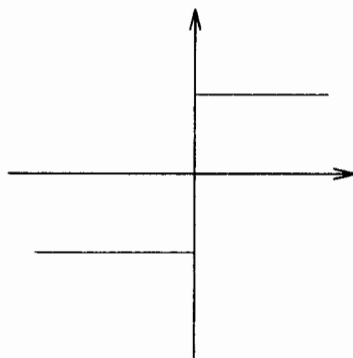


Figure 4.18: Switch nonlinearity.

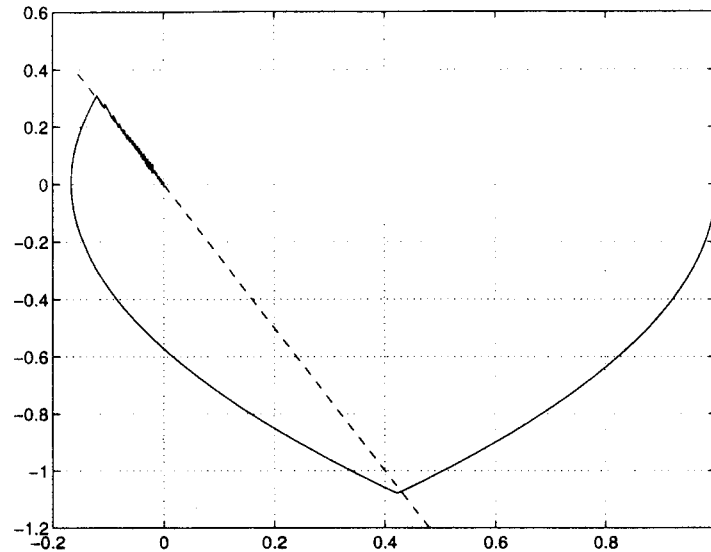


Figure 4.19: Phase portrait for on-off satellite control system.

among control engineers and forms the basis for all the “on-off” control methodologies. This is for example the case of many satellite control systems: Modelling one satellite axis as a double integrator

$$\ddot{\theta} = u,$$

we still combine a proportional plus derivative control logic with a switch to obtain the control law  $u = -\text{sgn}(\theta + 0.4\dot{\theta})$ . A typical trajectory for this system is shown in Fig 4.19. We see that several interesting phenomena occur: first, there actually is *no* equilibrium in the sense previously defined; nowhere does the vector field vanish to 0. However, trajectories seem to be converging towards 0 anyway, but in a very curious fashion: near the switching line (defined by  $\theta + 0.4\dot{\theta} = 0$ ), the vector field is such that it always tends to push the state on the other side of it, thus causing the system to “chatter” along the switching line until reaching 0, as seen in Fig. 4.20.

Such a behavior is unlike any encountered before, and its very existence is due to the switch discontinuity: switch is discontinuous. It is named the *sliding* phenomenon, and the switching line  $\theta + 0.4\dot{\theta}$  is named *sliding surface*. Depending on the application at hand, such a behavior may or may not be desirable. In any case, we see that starting in the

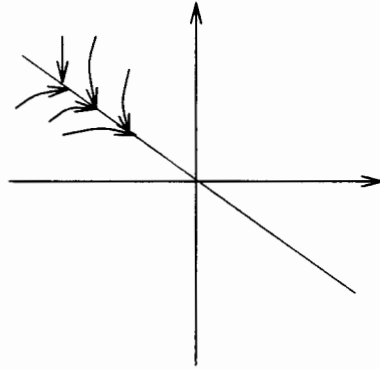


Figure 4.20: Sliding phenomenon

sliding surface, the behavior of the system is *linear and first-order* and satisfies the differential equation

$$\theta + 0.4\dot{\theta} = 0.$$

Note that these dynamics are *independent* from the original system's dynamics.

### Dry friction

Dry (or Coulomb) friction is extremely common in aerospace systems. It appears whenever two solids rub against each other, and is the cause for major trouble, by causing undesirable vibrations or blocking critical mechanisms, most recently in tethered satellite experiments. Consider first the simplest case of a Mass-Spring system with dry friction, as shown in Fig. 4.21. In the absence of friction, such a system is an harmonic oscillator. Subject to dry friction, this system is subject to a force which is constant in amplitude, but not in direction, as it is constantly opposed to the direction motion takes place. Thus, when motion takes place, dry friction amplitude is given by  $f_0 \text{sgn } \dot{x}$ , where  $\dot{x}$  is the speed of the system. Usually,  $f_0$  is proportional to the weight of the mass, according to the formula  $f_0 = \mu mg$ , where  $m$  is mass and  $g$  is gravity. When no motion occurs ( $\dot{x} = 0$ ), then the dry friction can assume any values between  $-f_0$  and  $f_0$ . In particular, if the spring tension  $-kx$  is less than  $f_0$  in amplitude, then dry friction will

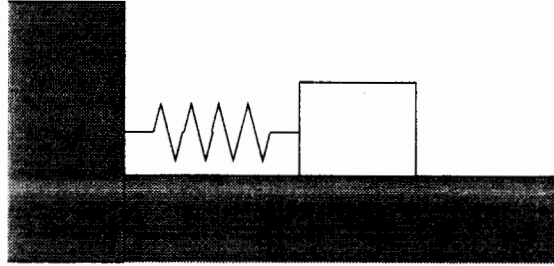


Figure 4.21: Mass-spring system subject to dry friction

exactly cancel this force such that equilibrium will happen. Otherwise, it will assume its maximum value, opposite to spring tension force. To summarize, dry friction is completely characterized by the system

$$\begin{cases} +f_0 & \text{for } \dot{x} < 0, \\ +f_0 & \text{for } \dot{x} = 0 \text{ and } kx > f_0 \\ +kx & \text{for } \dot{x} = 0 \text{ and } |kx| \leq f_0 \\ -f_0 & \text{for } \dot{x} = 0 \text{ and } kx < -f_0 \\ -f_0 & \text{for } \dot{x} > 0 \end{cases}$$

Thus, dry friction is a nonlinear force whose expression depends on speed as well as position of the mass. The equation of motion for the oscillator may be written as

$$m\ddot{x} + kx - f = 0.$$

When motion happen with positive speed ( $\dot{x} > 0$ ), then it is

$$m\ddot{x} + kx + f_0 = 0.$$

When speed is negative ( $\dot{x} < 0$ ), then the equation of motion becomes

$$m\ddot{x} + kx - f_0 = 0.$$

Thus, the phase portrait for nonzero velocities may simply be built from the phase portraits of two harmonic oscillators, whose equilibria are  $(-f_0/k, 0)$  and  $(f_0/k, 0)$ , respectively. The trajectories for these oscillators may be directly simulated, or obtained by rewriting the oscillator equations as

$$m \frac{d^2(x - f_0/k)}{dt^2} + k(x - f_0/k) = 0$$

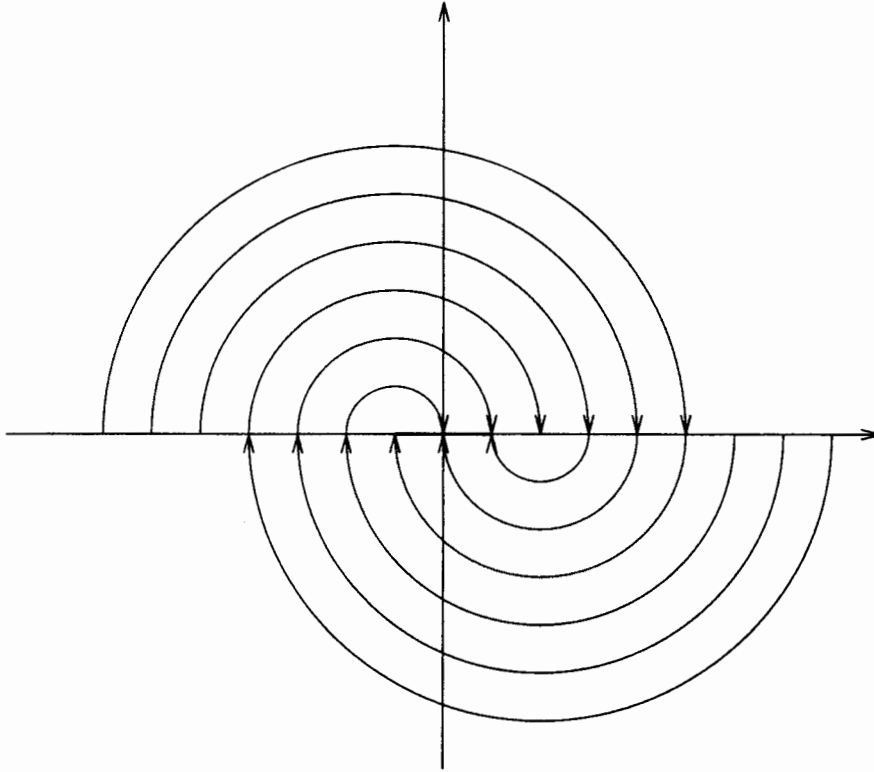


Figure 4.22: Phase-plane portrait for oscillator with dry friction

and

$$m \frac{d^2(x + f_0/k)}{dt^2} + k(x + f_0/k) = 0$$

respectively, and integrating them once to get

$$m \left( \frac{d(x - f_0/k)}{dt} \right)^2 + k(x - f_0/k)^2 = K,$$

and

$$m \left( \frac{d(x + f_0/k)}{dt} \right)^2 + k(x + f_0/k)^2 = K,$$

which are ellipsoids centered around the two equilibria. Thus, typical trajectories look like the ones shown in Fig. 4.22. The thickened segment in the picture represents the set of all possible equilibria. It is

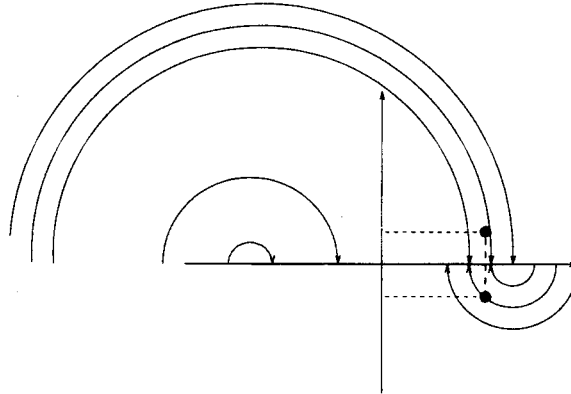


Figure 4.23: Relative effect of impulses in opposite directions

easy to see that trajectories are linearly decreasing, until they reach one equilibrium (in finite time). We also note that these equilibria are not all “equivalent”: Some of them are somewhat “unstable”; indeed, assume that a “dither” is repeatedly applied to the mass, that is, impulses of small and equal amplitudes are applied successively in both directions, letting the system go to rest afterwards. We see from Fig. 4.23 that one of the impulses will drive the mass away from zero, and the other will drive it nearer zero. However, the net motion is in favor of the motion towards zero. Thus, any equilibrium outside zero is sensitive to process noise (and dither is indeed a good way to get rid of dry friction).

Note that the presented dry friction model is not unique. In particular, dry friction tends to decay with speed, possibly with some discontinuities at 0. This is the case for dry friction/stiction models, where the static forces may actually be much higher than when motion occurs. Moreover, dry friction forces may change depending on which direction speed is going. This is the case if surfaces of contact look like the ones shown on Fig. 4.24. A more general format for dry friction may be then characterized by 4 elements: two stiction constants  $s^+$  and  $s^-$  and two decreasing friction functions  $f^+(\dot{x})$  and  $f^-(\dot{x})$  with  $f^+(0) \leq s^+$  and  $f^-(0) \leq s^-$ , such that, when expressed for the mass-spring system, the

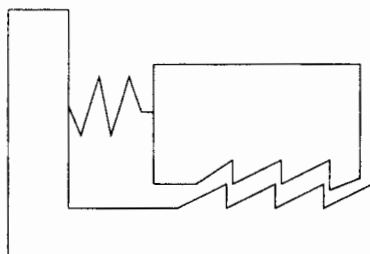


Figure 4.24: Asymmetric contact between surfaces.

friction force value is given by

$$\begin{cases} +f^-(\dot{x}) & \text{for } \dot{x} < 0, \\ +s^- & \text{for } \dot{x} = 0 \text{ and } kx > s^- \\ +kx & \text{for } \dot{x} = 0 \text{ and } s^- \geq kx \geq -s^+ \\ -s^+ & \text{for } \dot{x} = 0 \text{ and } kx < -s^+ \\ -f^+(\dot{x}) & \text{for } \dot{x} > 0 \end{cases}$$

### 4.3 Extensions

So far, we have studied systems with *static* nonlinearities, that is, systems where nonlinearities could be determined directly out of the state of the system. It turns out that this is not sufficient for many aerospace control applications. For example, satellite control strategies make heavy use of nonlinearities coupled with desired or undesired delays and hysteresis. Delays are systematically associated with real-life systems and may be encountered, for example, when switching jets on and off in satellite systems. The most common elements exhibiting hysteresis include *Schmitt triggers*, whose characteristics are shown in Fig. 4.25. It may be noted that these nonlinearities not only depend on current state, but on past values of the state as well. As a result, phase-plane analysis, though still very useful, is not as powerful as in the previous cases. In particular, uniqueness of trajectories passing through one given point is not ensured anymore. For example, consider the on-off satellite control system with a small time delay when firing thrusters, as shown in Fig. 4.26. The corresponding equations of motion are given

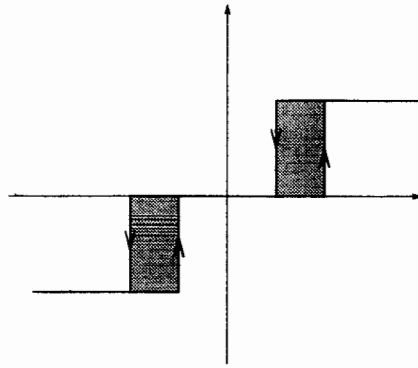


Figure 4.25: Schmitt Trigger.

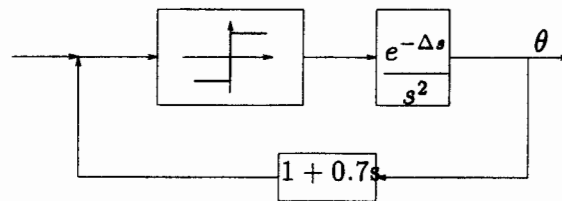


Figure 4.26: Block diagram for on-off satellite attitude control system with delay



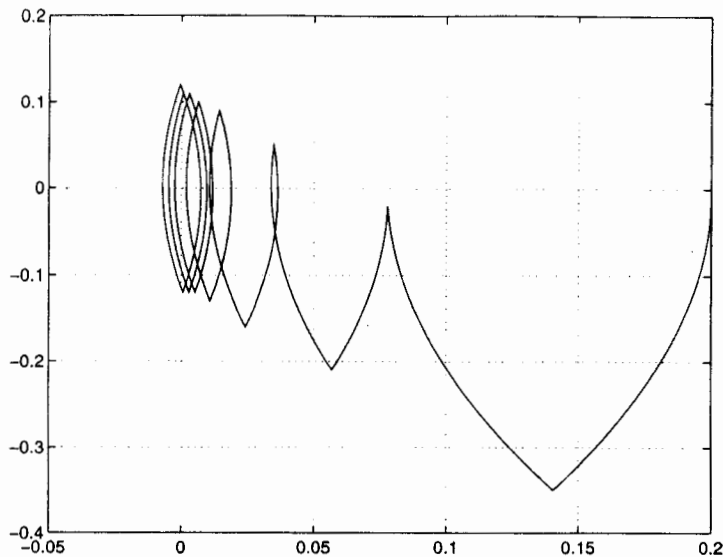


Figure 4.27: Phase portrait for on-off system and delay.

by

$$\ddot{\theta}(t) + \text{sgn}(\theta(t - \Delta) + 0.7\dot{\theta}(t - \Delta)) = 0.$$

In Fig. 4.27, we have plotted the response of this system in the canonical phase plane starting from the initial condition  $(0.2, 0)$ , and assuming that earlier controls were set to 0 (in order to obtain a value for the time delay). We see that through one point in the phase plane, there can now pass many trajectories, which end up in a limit cycle. The same phenomenon happens with Schmitt triggers.

## Problems

### 1. Dry friction on a beam with rotating supports

Consider the system shown in Fig. 4.28. The beam is subject to gravity, and it is resting on a pair of circular supports, as shown in Fig. 4.28. Under the effect of gravity, dry friction occurs at both points of contact, and when the beam (assumed to be homogenous, rectangular) is perfectly centered, the dry friction on both supports is characterized by the parameters  $s^+$ ,  $s^-$ ,  $f^+$ ,

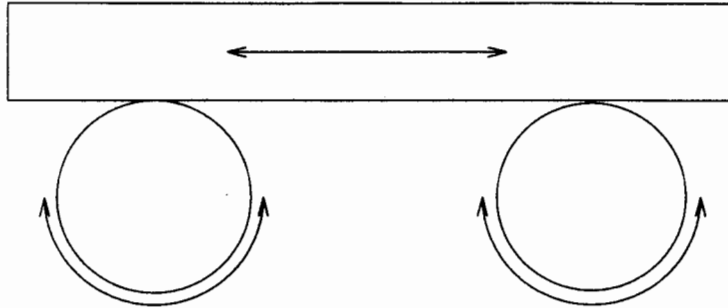


Figure 4.28: Beam on rotating supports

$f^-$  as in the notes. When the beam is offset, you know that the dry friction then varies *linearly* with the vertical load applied to each support.

- Assume the left wheel is rotating counterclockwise, and the right wheel is rotating clockwise. Draw the phase portrait for this system and also draw your conclusions.
- From now on, assume the left wheel is rotating clockwise, and the right wheel is rotating counterclockwise. Assume that  $f^+ = f^- = s^+ = s^-$ . Draw the phase portrait for this system.
- Assume now  $f^+$  and  $f^-$  are decreasing as  $e^{-\alpha|x|}$ . Can you describe the resulting motion as a function of  $\alpha$ ?

## 2. Dry friction and mass-spring systems

A mass is connected to a spring as shown in Fig. 4.29. The other end of the spring moves at a constant speed  $V$ . The mass is subject to dry friction.

- Describe the motion of the mass as  $V$  varies with  $s^+ = s^- = f^+ = f^-$ .
- Do the same assuming an exponentially decaying dry friction similar to the previous problem.

Based on this analysis, can you explain how violins and squeaking door hinges work?

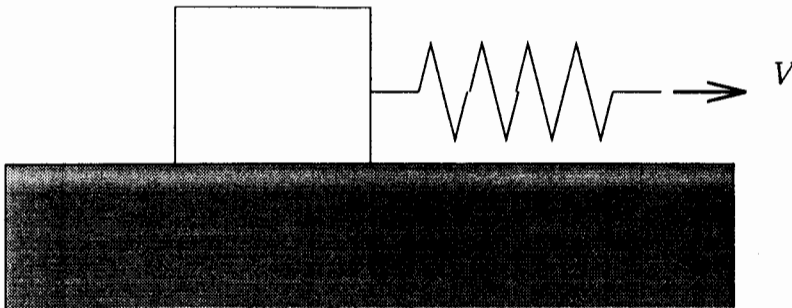
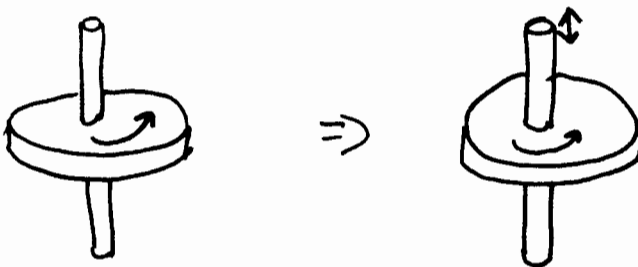


Figure 4.29: Mass-spring pulled at constant speed  $V$

3. **Transforming dry friction into viscous friction** Assume a rotating wheel is loosely mounted on an axis such that it may rotate and slide along that axis, with a given friction coefficient  $\mu$ .

- Assume the wheel cannot move along the axis. Describe its rotational motion.
- Assume now the wheel can rotate and the axis moves rapidly in and out of the wheel at constant relative speed  $V$ , as seen on the picture. Describe the rotational motion of the wheel.

This method is actually used in specific instruments subject to dry friction and is named a Brown arrangement.



4. **Predicting speed of convergence to 0 for piecewise linear, nonlinear system**

Consider a car with unit mass sliding on a line and powered with two opposing proportional jets, such that when the control  $u$  is positive, actual jet force is equal to  $u$ , and when  $u$  is negative, actual jet force is  $0.5u$ . Assume the control law  $u = -x - 0.2\dot{x}$  is used. Although this system is obviously stable, it cannot be linearized around zero. However, we can still say many things about it.

- Assume the canonical state-space. Draw a half line originating at 0. Given an initial condition right on that line, does the resulting trajectory cross that line again?
- How many simulations do you need to draw a general opinion about the previous question?
- Call your initial condition on that half line  $x_0$ . Then call the next crossing point  $x_1$ , etc... You have obtained a sequence of points. Can you draw general statements about this sequence?
- Compute the decay rate for this system.

The sequence you have just built is named a *Poincaré sequence*. It is central to the analysis of general nonlinear systems, and it may also be used to measure speed of convergence towards a limit cycle, for example.

### 5. Dry friction again!

Assume a mass, subject to dry friction, is at rest on a flat plate.

- Show that by vibrating the plate horizontally (net motion must be zero!) the mass can *climb* along the slope.
- Could you have done that with viscous friction?
- What if the plate is actually not horizontal?

This phenomenon is commonly used in industry to carry around small, identical items, via special vibrating devices named bowlfeeders.